Dalton Transactions

COMMUNICATION

View Article Online
View Journal | View Issue

Cite this: *Dalton Trans.*, 2015, **44**, 20312

Received 6th September 2015,
Accepted 13th October 2015

DOI: 10.1039/c5dt03463a

www.rsc.org/dalton

Silatranes for binding inorganic complexes to metal oxide surfaces†

Kelly L. Materna, Bradley J. Brennan and Gary W. Brudvig

A ruthenium complex containing silatrane functional groups has been synthesized and covalently bound to a conductive metal oxide film composed of nanoparticulate ITO (*nano*ITO). The silatrane-derived siloxane surface anchors were found to be stable in the examined range of pH 2 to 11 in aqueous phosphate buffer, and the ruthenium complex was found to have stable electrochemical features with repeated electrochemical cycling. The non-coordinating properties of the silatrane group to metals, which facilitates synthesis of silatrane-labeled coordination complexes, together with the facile surface-binding procedure, robustness of the surface linkages, and stability of the electrochemical properties suggest that incorporating silatrane motifs into ligands for inorganic complexes provides superior properties for attachment of catalysts to metal oxide surfaces under aqueous conditions.

Water-stable surface anchors for attachment of molecular complexes to metal oxides are needed for functional materials used in heterogeneous catalysis and aqueous photoelectrochemical devices.[1–8] Surfaces with immobilized inorganic compounds are of great importance for heterogeneous catalysis, especially for alternative energy applications where water oxidation and proton reduction catalysts are widely studied.[1,2,4–7,9–14] A range of artificial photosynthetic devices operate in water.[9,15–18] In addition, due to the varying pH stability profiles of components (catalysts, photosensitizers, electrodes, *etc.*) in these devices, systems need to be stable over a wide pH range in aqueous media. Recent developments to increase the stability of covalently bound dyes and catalysts onto metal oxide surfaces have involved using atomic layer deposition (ALD) of metal oxides as a protecting layer or by using water-stable surface anchoring groups linked to the molecules for strong surface attachment.[4,17,19,20]

Molecular precursors for surface-anchoring to metal oxides have been widely studied and include carboxylic acids, phosphonic acids, triethoxysilanes, acetylacetonate, hydroxamic acids, and silatranes.[1,4–7,13,14,21–23] Tripodal anchoring groups have been utilized due to their higher stability on surfaces.[2] Among water-stable anchoring groups, silatranes are of particular interest because they are non-protic, non-ionic, and form strong siloxane surface bonds to metal oxides. In addition, the caged trialkoxysilane precursor contains a pentacoordinate silicon atom, making the silatrane resistant to hydrolysis compared to the more commonly used non-caged silane analogues.[5,24,25] Porphyrins and Ru dyes containing silatrane groups have been bound to metal oxides for use in photoelectrochemical cells (PECs) and were found to have increased resistance to hydrolysis relative to phosphonic acids and carboxylic acids.[5,6] These features make the silatrane a promising anchoring group for binding inorganic complexes to metal oxides. The Ru complex **1** shown in Fig. 1 containing two silatrane groups was synthesized, and its behavior on high surface area films composed of nanoparticulate indium tin oxide (*nano*ITO) was studied. Complex **1** is a derivative of

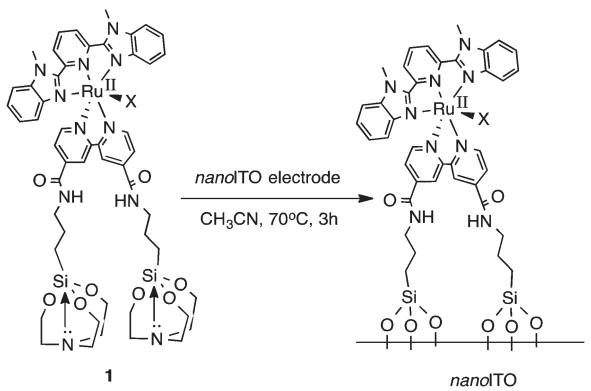

Fig. 1 Structure of Ru^{II}(Mebimpy)(bpy-Sil)X, (**1**) and its proposed surface-binding mode on *nano*ITO electrodes. X = solvent, bpy-Sil = 2,2′-bipyridine-4,4′-diamidopropylsilatrane, Mebimpy = 2,6-bis(1-methylbenzimidazole-2-yl)pyridine.

Energy Sciences Institute and Department of Chemistry, Yale University, P.O. Box 208107, New Haven, CT 06520-8107, USA

†Electronic supplementary information (ESI) available: Supplementary experimental information and data (Fig. S1–S5 and Table S1). See DOI: 10.1039/c5dt03463a

[Ru(Mebimpy)(bpy)Cl]Cl, Mebimpy = 2,6-bis(1-methylbenzimidazole-2-yl)pyridine and bpy = 2,2′-bipyridine, that has been reported as a water-oxidation catalyst in homogeneous solution[26] as well as a heterogenized catalyst using phosphonate anchoring groups to a metal oxide surface.[1] This complex was chosen as a model catalyst containing an exchangeable coordination site on Ru to show the practicality of incorporating silatranes into inorganic complexes for covalent binding to metal oxide surfaces. The silatrane group is shown to not only provide excellent stability for anchoring an inorganic coordination compound to a metal oxide surface but also to enable synthesis of the inorganic complex-silatrane conjugate without complications from binding of the anchoring group to the metal center of the complex.

Complex **1** was synthesized by modifying a procedure[26] for the synthesis of [Ru(Mebimpy)(bpy)Cl]Cl by substituting the bpy ligand for a bpy-silatrane (bpy-Sil) ligand during the synthesis. The bpy-Sil ligand precursors were prepared by a known procedure.[5] Complex **1** was prepared by stirring [Ru(Mebimpy)(bpy-Sil)Cl]Cl in MeOH with $AgNO_3$ overnight and filtering off the resulting AgCl; further synthetic details can be found in the ESI.† Interestingly, the silatrane functional group did not decompose or react with the ruthenium metal center during the synthesis of **1**. As surface-anchoring functional groups are designed to chelate metals, stability during formation of an inorganic complex is crucial. Functional groups with strong metal oxide binding, such as hydroxamic acids, have been found to be incompatible during synthesis of some metal complexes due to their strong propensity to chelate.[7,27] The silatrane is protected from these side-reactions due to its caged structure.

Meyer and coworkers have previously reported enhanced rates of water oxidation for ruthenium water-oxidation catalysts covalently bound using phosphonate anchoring groups to *nano*ITO electrodes.[1] The *nano*ITO electrodes aid in the higher rates since they are a high surface area nanoparticulate material; they are also optically transparent and have a high electrical conductivity. As a result, catalyst-chromophore assemblies have been developed using these electrodes.[1,11,28–30] Conductive *nano*ITO electrodes composed of sintered nanoparticles on a fluorinated tin oxide (FTO) substrate were prepared by known methods[22,28] and were functionalized by soaking in a 0.3 mM solution of **1** for three hours at 70 °C; the proposed surface attachment can be seen in Fig. 1. After three hours, the surface coverage of complex **1** was calculated from UV-visible spectroscopic measurements using $\Gamma = A(\lambda)/(\varepsilon(\lambda) \times 10^3)$, where A and ε are the absorbance and molar absorptivities at wavelength λ = 479 nm. The molar absorptivity, ε(479 nm) = 8430 M^{-1} cm^{-1}, was based on measurements of complex **1** in acetonitrile; molar absorptivity data can be found in the ESI (Fig. S1†). Approximately 35 nmol cm^{-2} was found to be the surface coverage after three hours, which agrees with the saturated surface coverages of the previously reported phosphonate anchored complex.[1] The silatrane cage deprotects on the metal oxide surface to form siloxyl bonds as described previously.[6] Deprotection of the silatrane has been shown to occur on both TiO_2 and SnO_2 surfaces.[5]

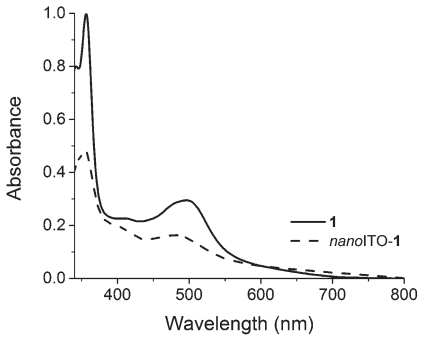

Fig. 2 UV-visible absorbance spectra of complex **1** in acetonitrile (—) and bound to *nano*ITO (---).

Fig. 2 shows the UV-visible spectra of the *nano*ITO electrodes sensitized with complex **1** (*nano*ITO-1) and complex **1** dissolved in acetonitrile. The spectra have nearly identical features, although the absorption peaks are somewhat broadened in the *nano*ITO-1 spectrum due to light scattering in the film. The similarities suggest that the molecular structure on the surface has not changed upon surface adsorption.

Cyclic voltammetry (CV) of the functionalized electrode *nano*ITO-1 was performed in phosphate-buffered aqueous solutions from pH 2 to 11. The CVs of *nano*ITO-1 at pH 7 with varying scan rates are shown in Fig. 3. The electrochemical data collected under the remaining pH conditions can be found in the ESI (Fig. S2†). Three distinct redox features were observed with midpoint potentials that agree with those of similar ruthenium complexes.[1] The redox feature at 0.45 V *vs.* NHE at pH 7 has been described as a $Ru^{IV}(OO)^{2+}/Ru^{III}(OOH)^{2+}$ or Ru^{III}-$(OOH)^{2+}/Ru^{II}(HOOH)^{2+}$ intermediate that forms in an aqueous environment; this has been observed with a similarly ligated ruthenium water-oxidation catalyst.[1,31] This feature is only observed after the first voltametric cycle. The second feature at 0.77 V is due to the $Ru^{II/III}$ couple, and the third feature at 1.16 V is due to the $Ru^{III/IV}$ couple.[1] Fig. 3 (as well as Fig. S2 and Table S1†) indicates that anodic and cathodic peak separations approach 0 mV as scan rates decrease under all pH conditions, suggesting that **1** is a surface-bound species. Further evidence for a surface species is shown in Fig. 3 (and Fig. S2†) where plots of scan rate *vs.* anodic peak Faradaic current are linear.

The $Ru^{II/III}$ and $Ru^{III/IV}$ midpoint potentials were found to vary with pH, but less than the theoretical 59 mV/pH unit (Table S1†).[1] The complicated effects of electrolyte anions on electrochemical analyses have been previously studied, and these are likely to be playing a role in our electrochemical features.[32,33]

Hydrolytic and chemical stability of the ruthenium complex were examined by repeated CV cycling in aqueous buffered phosphate solutions at pH 7, 8 and 11 (Fig. S3†). Under all conditions, the redox features remained consistent in their midpoint potentials, ratio and intensity, suggesting that compound **1** is both chemically stable under these alkaline con-

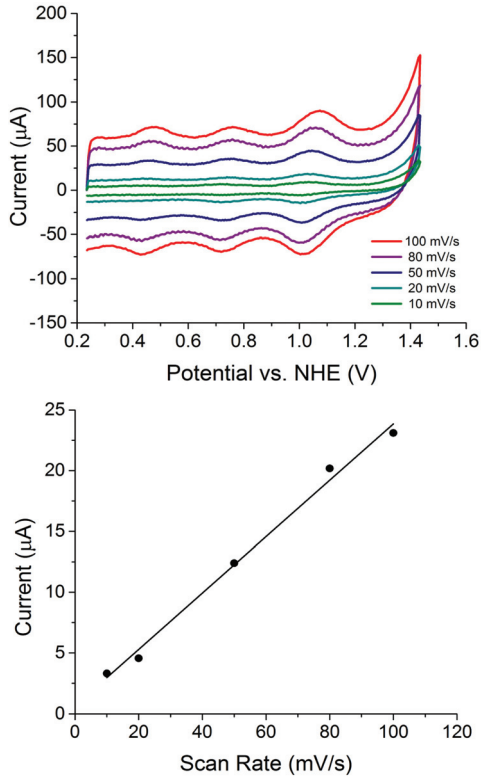

Fig. 3 Top: Cyclic voltammograms of *nano*ITO-1 at pH = 7 with scan rates 100 mV s^{-1} (red), 80 mV s^{-1} (purple), 50 mV s^{-1} (blue), 20 mV s^{-1} (teal), and 10 mV s^{-1} (green); bottom: scan rate *vs.* peak Faradaic current for *nano*ITO-1 (R^2 = 0.996).

ditions and very strongly bound to the *nano*ITO electrode. A 100 mV s^{-1} scan rate was chosen for this experiment because this provided the most resolved redox features.

To further show the stability of the anchored complex, CVs of the phosphate electrolyte at pH 2 and pH 11 were performed using a *nano*ITO blank electrode after 30 minute electrolyses of *nano*ITO-1 with a 1.4 V *vs.* NHE applied bias. These CVs were compared to fresh phosphate electrolyte and were found to be identical. This provides further evidence that complex **1** remained surface bound and did not appreciably leach into the electrolyte during electrolysis (Fig. S4†). Compared with carboxylate and phosphonate anchoring groups, silatranes make an excellent surface anchoring group due to their stability under acidic, neutral, and basic conditions.[3,34,35]

Complexes that can be characterized pre- and post-surface binding aid in characterizing the surface-bound complex.[1,4,10] UV-visible spectra, shown in Fig. 2, and cyclic voltammetry of **1** on *nano*ITO (Fig. 3 and S2†) and in solution (Fig. S5†) help support the hypothesized surface structure. The silatrane precursor is electrochemically stable in solution, and has similar redox features to the surface-bound complex. These comparisons provide a good basis for understanding the surface-bound ruthenium complex.

Conclusions

Here we showed the use of the silatrane functional group to bind an inorganic complex to a metal oxide surface. From the above synthetic and electrochemical results, it is evident that incorporating silatrane groups into ligands can be a useful way to bind inorganic transition metal complexes to surfaces due to the non-reactivity of silatranes with metal centers during synthesis, their ability to form strong surface bonds to metal oxides that are resistant to hydrolysis, and their electrochemical stability. The pH stability range of silatranes has not yet been completely established, as we did not observe loss of surface-bound material during our experiments between pH 2 and 11; the limits of the siloxane surface-bond stability in water is being further investigated. These favorable characteristics of silatranes make them a great addition to the field of heterogeneous catalysis. Additional analyses of silatrane surface binding to metal oxide surfaces and applications are currently ongoing.

Acknowledgements

This work was funded by U.S. Department of Energy Grant DE-FG02-07ER15909 and a generous gift from the TomKat Charitable Trust.

Notes and references

1 Z. Chen, J. J. Concepcion, J. F. Hull, P. G. Hoertz and T. J. Meyer, *Dalton Trans.*, 2010, **39**, 6950–6952.
2 E. Galoppini, *Coord. Chem. Rev.*, 2004, **248**, 1283–1297.
3 I. Gillaizeau-Gauthier, F. Odobel, M. Alebbi, R. Argazzi, E. Costa, C. A. Bignozzi, P. Qu and G. J. Meyer, *Inorg. Chem.*, 2001, **40**, 6073–6079.
4 W. R. McNamara, R. L. Milot, H.-e. Song, R. C. Snoeberger III, V. S. Batista, C. A. Schmuttenmaer, G. W. Brudvig and R. H. Crabtree, *Energy Environ. Sci.*, 2010, **3**, 917–923.
5 B. J. Brennan, A. E. Keirstead, P. A. Liddell, S. A. Vail, T. A. Moore, A. L. Moore and D. Gust, *Nanotechnology*, 2009, **20**, 505203.
6 B. J. Brennan, M. J. Llansola Portoles, P. A. Liddell, T. A. Moore, A. L. Moore and D. Gust, *Phys. Chem. Chem. Phys.*, 2013, **15**, 16605–16614.
7 T. P. Brewster, S. J. Konezny, S. W. Sheehan, L. A. Martini, C. A. Schmuttenmaer, V. S. Batista and R. H. Crabtree, *Inorg. Chem.*, 2013, **52**, 6752–6764.
8 K. J. Young, L. A. Martini, R. L. Milot, R. C. Snoeberger III, V. S. Batista, C. A. Schmuttenmaer, R. H. Crabtree and G. W. Brudvig, *Coord. Chem. Rev.*, 2012, **256**, 2503–2520.
9 H. I. Karunadasa, C. J. Chang and J. R. Long, *Nature*, 2010, **464**, 1329–1333.
10 W. R. McNamara, R. C. Snoeberger 3rd, G. Li, J. M. Schleicher, C. W. Cady, M. Poyatos,

C. A. Schmuttenmaer, R. H. Crabtree, G. W. Brudvig and V. S. Batista, *J. Am. Chem. Soc.*, 2008, **130**, 14329–14338.
11 M. R. Norris, J. J. Concepcion, Z. Fang, J. L. Templeton and T. J. Meyer, *Angew. Chem., Int. Ed.*, 2013, **52**, 13580–13583.
12 M. R. Norris, J. J. Concepcion, C. R. Glasson, Z. Fang, A. M. Lapides, D. L. Ashford, J. L. Templeton and T. J. Meyer, *Inorg. Chem.*, 2013, **52**, 12492–12501.
13 Y. Gao, X. Ding, J. Liu, L. Wang, Z. Lu, L. Li and L. Sun, *J. Am. Chem. Soc.*, 2013, **135**, 4219–4222.
14 V. Singh, P. C. Mondal, M. Chhatwal, Y. L. Jeyachandran and M. Zharnikov, *RSC Adv.*, 2014, **4**, 23168–23176.
15 S. W. Sheehan, J. M. Thomsen, U. Hintermair, R. H. Crabtree, G. W. Brudvig and C. A. Schmuttenmaer, *Nat. Commun.*, 2015, **6**, 6469.
16 A. J. Bloomfield, S. W. Sheehan, S. L. Collom, R. H. Crabtree and P. T. Anastas, *New J. Chem.*, 2014, **38**, 1540–1545.
17 L. Wang, M. Mirmohades, A. Brown, L. Duan, F. Li, Q. Daniel, R. Lomoth, L. Sun and L. Hammarström, *Inorg. Chem.*, 2015, **54**, 2742–2751.
18 S. Berardi, S. Drouet, L. Francas, C. Gimbert-Surinach, M. Guttentag, C. Richmond, T. Stoll and A. Llobet, *Chem. Soc. Rev.*, 2014, **43**, 7501–7519.
19 K. Hanson, M. D. Losego, B. Kalanyan, G. N. Parsons and T. J. Meyer, *Nano Lett.*, 2013, **13**, 4802–4809.
20 A. K. Vannucci, L. Alibabaei, M. D. Losego, J. J. Concepcion, B. Kalanyan, G. N. Parsons and T. J. Meyer, *Proc. Natl. Acad. Sci. U. S. A.*, 2013, **110**, 20918–20922.
21 Y. Gao, L. Zhang, X. Ding and L. Sun, *Phys. Chem. Chem. Phys.*, 2014, **16**, 12008–12013.
22 B. H. Farnum, Z. A. Morseth, A. M. Lapides, A. J. Rieth, P. G. Hoertz, M. K. Brennaman, J. M. Papanikolas and T. J. Meyer, *J. Am. Chem. Soc.*, 2014, **136**, 2208–2211.
23 W. R. McNamara, R. C. Snoeberger III, G. Li, C. Richter, L. J. Allen, R. L. Milot, C. A. Schmuttenmaer, R. H. Crabtree, G. W. Brudvig and V. S. Batista, *Energy Environ. Sci.*, 2009, **2**, 1173–1175.
24 B. J. Brennan, D. Gust and G. W. Brudvig, *Tetrahedron Lett.*, 2014, **55**, 1062–1064.
25 C. L. Frye, G. A. Vincent and W. A. Finzel, *J. Am. Chem. Soc.*, 1971, **93**, 6805–6811.
26 J. J. Concepcion, M. K. Tsai, J. T. Muckerman and T. J. Meyer, *J. Am. Chem. Soc.*, 2010, **132**, 1545–1557.
27 U. Mollmann, L. Heinisch, A. Bauernfeind, T. Kohler and D. Ankel-Fuchs, *Biometals*, 2009, **22**, 615–624.
28 P. G. Hoertz, Z. Chen, C. A. Kent and T. J. Meyer, *Inorg. Chem.*, 2010, **49**, 8179–8181.
29 W. Song, C. R. K. Glasson, H. Luo, K. Hanson, M. K. Brennaman, J. J. Concepcion and T. J. Meyer, *J. Phys. Chem. Lett.*, 2011, **2**, 1808–1813.
30 D. K. Zhong, S. Zhao, D. E. Polyansky and E. Fujita, *J. Catal.*, 2013, **307**, 140–147.
31 Z. Chen, J. J. Concepcion, J. W. Jurss and T. J. Meyer, *J. Am. Chem. Soc.*, 2009, **131**, 15580–15581.
32 Z. Chen, J. J. Concepcion, X. Hu, W. Yang, P. G. Hoertz and T. J. Meyer, *Proc. Natl. Acad. Sci. U. S. A.*, 2010, **107**, 7225–7229.
33 Y. Tamaki, A. K. Vannucci, C. J. Dares, R. A. Binstead and T. J. Meyer, *J. Am. Chem. Soc.*, 2014, **136**, 6854–6857.
34 D. G. Brown, P. A. Schauer, J. Borau-Garcia, B. R. Fancy and C. P. Berlinguette, *J. Am. Chem. Soc.*, 2013, **135**, 1692–1695.
35 K. Hanson, M. K. Brennaman, H. Luo, C. R. Glasson, J. J. Concepcion, W. Song and T. J. Meyer, *ACS Appl. Mater. Interfaces*, 2012, **4**, 1462–1469.